

The optical and electrical properties of Eu^{3+} - Y^{3+} codoped ITO transparent conductive electrodes as luminescent solar concentrators

C.-C. Ting & C.-H. Tsai

*Graduate Institute of Opto-Mechatronics Engineering,
National Chung Cheng University, Taiwan*

Abstract

Rare earth ions (Eu^{3+}) and Y^{3+} ions were codoped into the tin-doped indium oxide (ITO) transparent conductive electrode to make it possess visible luminescent properties. The Eu^{3+} - Y^{3+} codoped transparent conductive thin films with the precise control on the desired stoichiometry of dopants were fabricated by sol-gel spin-coating technologies. We first report that the Eu^{3+} - Y^{3+} codoped ITO thin films show better visible luminescent properties than Eu^{3+} -doped ITO thin films. The higher Y^{3+} concentration can increase the 611 nm PL intensity of Eu^{3+} - Y^{3+} codoped ITO thin films. However, the Eu^{3+} and Y^{3+} codoping concentrations should be controlled within 0.1% and 0.5%, respectively, to avoid the deterioration of conductivity. We believe that the Eu^{3+} - Y^{3+} codoped ITO thin films can play dual roles as the luminescent solar concentrators and transparent conductive electrode to enhance the efficiency of solar cells.

Keywords: ITO, europium, yttrium, pyrochlore, photoluminescence.

1 Introduction

The luminescent solar concentrators (LSC) have attracted lots of attention for the efficiency enhancement of solar cell these past years [1–3]. Most of the LSC is the organic or inorganic fluorescent materials which were coated on the surface of solar cell devices [4–6]. However, this kind of LSC will increase the manufacturing procedures and cost. There is only 5% ultraviolet (UV) and near blue light (300~400 nm) that can reach the Earth surface [7] and most of the solar cells do not have good operating efficiency in this section because of the



absorption of transparent conductive electrode [8, 9]. Therefore we hope that the luminescent solar concentrators can convert this UV light to 500~700 nm visible light, which can be further absorbed by solar cell.

In this study, we try to codope Eu^{3+} and Y^{3+} ions into the transparent conductive electrode, tin-doped indium oxide (ITO), to make them possess visible luminescent properties. These Eu^{3+} - Y^{3+} codoped ITO thin films with the precise control on the desired stoichiometry of dopants were fabricated by sol-gel spin-coating technologies. In order to maintain the conductivity of Eu^{3+} - Y^{3+} codoped ITO thin films, the doping concentrations of Eu^{3+} and Y^{3+} ions were kept at a low contents, i.e. Eu^{3+} (0.1 mol%) and Y^{3+} (0~4 mol%). Optical and electrical properties such as fluorescence and sheet resistance (ohms/square) of the resulting Eu^{3+} -doped ITO system were systematically examined in terms of the codoping concentrations and structural evolution of the films at 600°C annealing for 1 h.

2 Experiments

2.1 Preparation of precursor solutions

The precursor solutions for the fabrication of Eu^{3+} - Y^{3+} codoped ITO thin films and powders were synthesized by following procedures. The starting materials is anhydrous indium trichloride (InCl_3 , 99.995%, Acros) which was dissolved in the mixture of acetic acid (HAc, CH_3COOH , 99.5%, Acros) and 2-methoxyethanol (2-MOE, $\text{C}_3\text{H}_8\text{O}$, 99.5%, Merck) with molar ratio of $\text{In}/\text{HAc}/2\text{-MOE}=1/20/12$. Then the solution was refluxed at 80°C for 3 h. Anhydrous tin chloride (SnCl_4 , 99%, Acros) was dissolved in ethanol ($\text{C}_2\text{H}_5\text{OH}$, 99.9%, JT-Baker), which was dropped into the refluxed indium solution at room temperature.

Finally, the yttrium acetate [$\text{Y}(\text{CH}_3\text{COO})_3 \cdot 4\text{H}_2\text{O}$, 99.9%, Alfa] and europium nitrate [$\text{Eu}(\text{NO}_3)_3 \cdot 6\text{H}_2\text{O}$, 99.9%, Alfa] were dissolved in the solution (a mixture of methanol (CH_3OH , $\geq 99.5\%$, Merck) and ethylene glycol ($\text{HOCH}_2\text{CH}(\text{OH})\text{CH}_2\text{OH}$, $\geq 99.5\%$, Alfa)], which was added into the above-mentioned ITO solution and followed by stirring for 10 h at room temperature in order to process homogeneous hydrolysis and polymerization reaction. The molar ratio of Eu/In and Y/In varied from 0.05/100 to 0.2/100 and 0.5/100 to 4/100, respectively.

2.2 Preparation of thin-film coatings

All of the thin films were prepared by sol-gel spin-coating method in a class 100 clean bench. The Eu^{3+} - Y^{3+} codoped ITO precursor solutions were spin-coated on silica glass substrates of 25 mm×25 mm×0.6 mm dimension (Corning, Eagle 2000). The as-deposited sol-gel films were first dried at 100°C for 10 min, and pyrolyzed in air at 400°C for 10 min at a heating rate of 10°C/min. Finally, the as-formed films were annealed at different temperatures ranging from



600-1000°C for 1 h in air. Multiple spin-coating processes were employed to deposit ~300 nm thick films.

2.3 Characteristic measurements

The crystal structure was determined by an X-ray diffractometer (Shimadzu, XRD 6000). Scanning electron microscopy (Hitachi, S4800-I) was used for microstructural examination. The thickness of Eu^{3+} -doped ITO films was measured by the SEM cross-sectional image. A monochromator (Horiba Jobin-yvon, MicroHr) equipped with 300 W Xe lamp (Hamamatsu, L2479) and a 325 nm He-Cd laser with an output power of 4 mW were used as the excitation light source. The visible fluorescence was detected by spectrophotometer (Horiba Jobin-yvon, iHR 550) equipped with a PMT detector (Hamamatsu, 7732P-01) at room temperature. Resistivity of the films was measured by using the four-point probe method (Fluke, 8845A).

3 Results and discussions

3.1 Crystal structures and film morphologies

Figure 1 shows the XRD patterns of ITO film and Eu^{3+} (0.1 mol%)- Y^{3+} (0, 0.5, 1, 2, and 4 mol%) codoped ITO thin films annealed at 600°C for 1 h. All of the samples possessed the well-crystallized bixbyite phase identified by the characteristic XRD peaks: (222), (400), (440), and (622) [10]. Compared to the diffraction intensity of (222) peak between all samples, the addition of 0.5 mol% Eu^{3+} and 0.5-4 mol% Y^{3+} ions did not obviously influence the peak intensity of Eu^{3+} - Y^{3+} codoped ITO thin films, which implies that the slight addition of Eu^{3+} and Y^{3+} ions with a total concentration of up to 4.1 mol% into the ITO host did not significantly degrade the crystallinity of ITO thin films. The average crystal size was determined by the Scherrer's equation depending on the full width at half maximum (FWHM) of XRD peak [11]. For ITO film and Eu^{3+} (0.1 mol%)- Y^{3+} (1 mol%) codoped ITO thin films annealed at 600°C for 1 h, the FWHM of (222) peak increased from 0.336° to 0.466° and the average crystal sizes decreased from ~22 to ~19 nm.

On the other hand, all XRD patterns indicate the formation of single bixbyite-structured phase for Eu^{3+} - Y^{3+} codoped ITO thin films without any possible other phases such as Y_2O_3 , Eu_2O_3 , SnO_2 , $\text{In}_4\text{Sn}_3\text{O}_{12}$, and $\text{Y}_2\text{Sn}_2\text{O}_7$. ITO is a kind of solid solution which Sn^{4+} concentration of up to 10 mol% can dissolve in In_2O_3 lattice, resulting in the maximum conductivity [12]. Moreover, In_2O_3 , Y_2O_3 , and Eu_2O_3 possessed the same structures, *i.e.*, bixbyite phase and similar lattice constants (a), as summarized in Table I. Although Eu^{3+} and Y^{3+} ions in In_2O_3 lattice to form the solid solution *i.e.*, $\text{Y}_x\text{In}_{2-x}\text{O}_3$ and $\text{Eu}_x\text{In}_{2-x}\text{O}_3$. On the other hand, Eu_2O_3 and Y_2O_3 can react with SnO_2 to form the cubic pyrochlore phase, $\text{Y}_2\text{Sn}_2\text{O}_7$ and $\text{Eu}_2\text{Sn}_2\text{O}_7$. A. Ambrosini *et al.* investigated that by doping Y^{3+} ions into In_2O_3 lattice, the lattice constant can be enlarged because of Y^{3+} ions has larger radius than that of In^{3+} ions, which indicates the formation



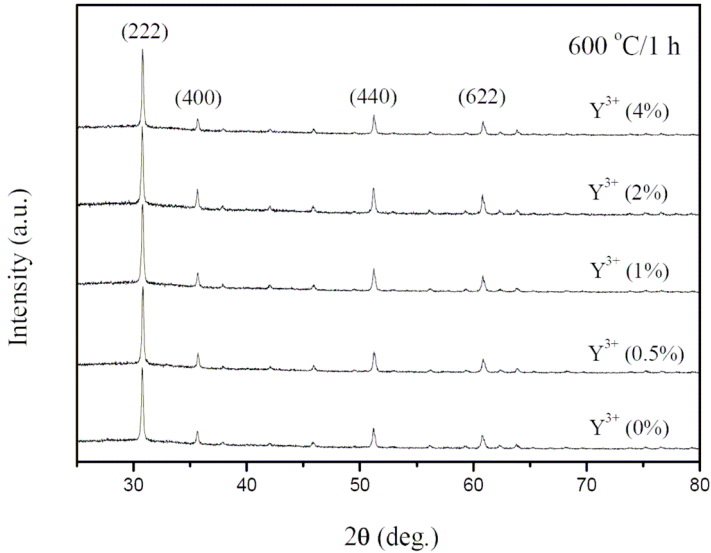


Figure 1: XRD patterns of ITO film and Eu^{3+} (0.1 mol%)- Y^{3+} (0, 0.5, 1, 2, and 4 mol%) codoped ITO thin films annealed at 600°C for 1 h.

Table 1: Ionic radii and crystallographic data of possible metal oxides in Eu^{3+} - Y^{3+} codoped ITO thin films.

Oxide	Lattice parameters (Å)	Metal ionic radius(Å)	Structure type	Reference
In_2O_3	$a = 10.11$	0.80	Bixbyite	PCPDF # 44-1087
Y_2O_3	$a = 10.60$	0.90	Bixbyite	PCPDF # 43-1036
SnO_2	$a = 4.74$ $c = 3.19$	0.69	Rutile	PCPDF # 41-1445
Eu_2O_3	$a = 10.86$	0.95	Bixbyite	PCPDF # 43-1008
$\text{Y}_2\text{Sn}_2\text{O}_7$	$a = 10.37$	1.02	Pyrochlore	PCPDF # 20-1418
$\text{In}_4\text{Sn}_3\text{O}_{12}$	$a = 9.46$ $c = 8.86$	-----	Delta	[21]

of solid solution $\text{Y}_y\text{In}_{2-y}\text{O}_3$. In addition, any available Y_2O_3 and SnO_2 in the Y^{3+} -doped ITO system can react with each other to form $\text{Y}_2\text{Sn}_2\text{O}_7$ until one of the starting materials is completely depleted. The formation of pyrochlore $\text{Y}_2\text{Sn}_2\text{O}_7$ at 1400°C annealing was detected by XRD even though the content of Y^{3+} ions is as low as 2 mol% in a Sn^{3+} -doped In_2O_3 pellet [13]. Fujihara *et al.* [14] reported that sol-gel derived $\text{Y}_2\text{Sn}_2\text{O}_7$ thin films were in amorphous state for $500\sim 700^\circ\text{C}$

annealing; however, the well-defined pyrochlore $Y_2Sn_2O_7$ thin films were obtained at 800°C or higher annealing temperatures. In our system, annealing temperature was 600°C and hence, the amorphous pyrochlore $Y_2Sn_2O_7$ can not crystallize to be detected by XRD. Park *et al.* [15] observed that the pyrochlore phase $Eu_2Sn_2O_7$ was detected in the Eu^{3+} -doped SnO_2 thin films annealed at 1200°C for 1 h while the doping concentration reached to 3 mol% [15].

In our experiment even though the light codoping concentration of Eu^{3+} and Y^{3+} ions is as low as ~4 mol%, the pyrochlore phase should be detected if it forms. However, there is no pyrochlore phase can be detected in Eu^{3+} - Y^{3+} codoped ITO thin films annealed at 600°C for 1 h. Based on the above-mentioned reported literatures, therefore, the Eu^{3+} (0.1 mol%)- Y^{3+} (0, 0.5, 1, 2, and 4 mol%) codoped ITO thin films annealed at 600°C for 1 h could be composed of the mixture of amorphous $Eu_xY_ySn_{2-x-y}O_7$ and crystallized $In_{2-z}Sn_zO_{3-\delta}$ (δ : oxygen vacancies) phases.

3.2 Fluorescent properties

Fluorescence intensity of the Eu^{3+} - Y^{3+} codoped ITO thin films with thickness of ~300 nm were found to be extremely low by the excitation of monochromator equipped with 300 W Xe lamp, which could not be detected due to the limitation of our existing spectrophotometer measurement set-up. However, when the film thickness was up to ~900 nm, the fluorescence intensity was stronger enough to be detected by monochromator excitation. The ~900 nm thick film appeared to have some cracks, which can not be used for the measurement of sheet resistance but can be used for the measurement of excitation spectrum. Therefore, the fluorescent measurement of all samples with thickness of ~300 nm was executed by using a 325 nm He-Cd laser with an output power of 4 mW as the excitation light source.

Figure 2 shows the emission fluorescence spectra of (a) Eu^{3+} (0.1 mol%)- Y^{3+} (0, 0.5, 1, 2, and 4 mol%) and (b) Eu^{3+} (0.05, 0.1, and 0.2 mol%)- Y^{3+} (1 mol%) codoped ITO thin films annealed at 600°C for 1 h. Obviously, the Eu^{3+} ions show only one characteristic visible emission, 611 nm red light, which is attributed to the ${}^5D_0 \rightarrow {}^7F_2$ transition of Eu^{3+} ions. Interestingly, no ${}^5D_0 \rightarrow {}^7F_1$ transition (~590 nm) of Eu^{3+} ions can be detected for all samples. It is well known that the probability of intra-4f-f transitions strongly depends on the site

The electric-dipole ${}^5D_0 \rightarrow {}^7F_2$ transition is allowed for the Eu^{3+} site without inversion symmetry. On the other hand, the Eu^{3+} ions can exhibit the magnetic-dipole ${}^5D_0 \rightarrow {}^7F_1$ transition because of the Eu^{3+} site with inversion symmetry [16]. In general, both of the electric-dipole and magnetic-dipole transitions coexist in the fluorescent spectra of many Eu^{3+} -doped inorganic materials but one is always much stronger than the other. Further, the intensity ratio of the electric-dipole and magnetic-dipole transitions can be used to investigate the asymmetry of Eu^{3+} ions in the host lattice site [16]. It is reasonable that only electric-dipole ${}^5D_0 \rightarrow {}^7F_2$ transition was observed in our system because Eu^{3+} ions is located in the amorphous $Eu_xY_ySn_{2-x-y}O_7$ lattice site which results in reducing site symmetry of

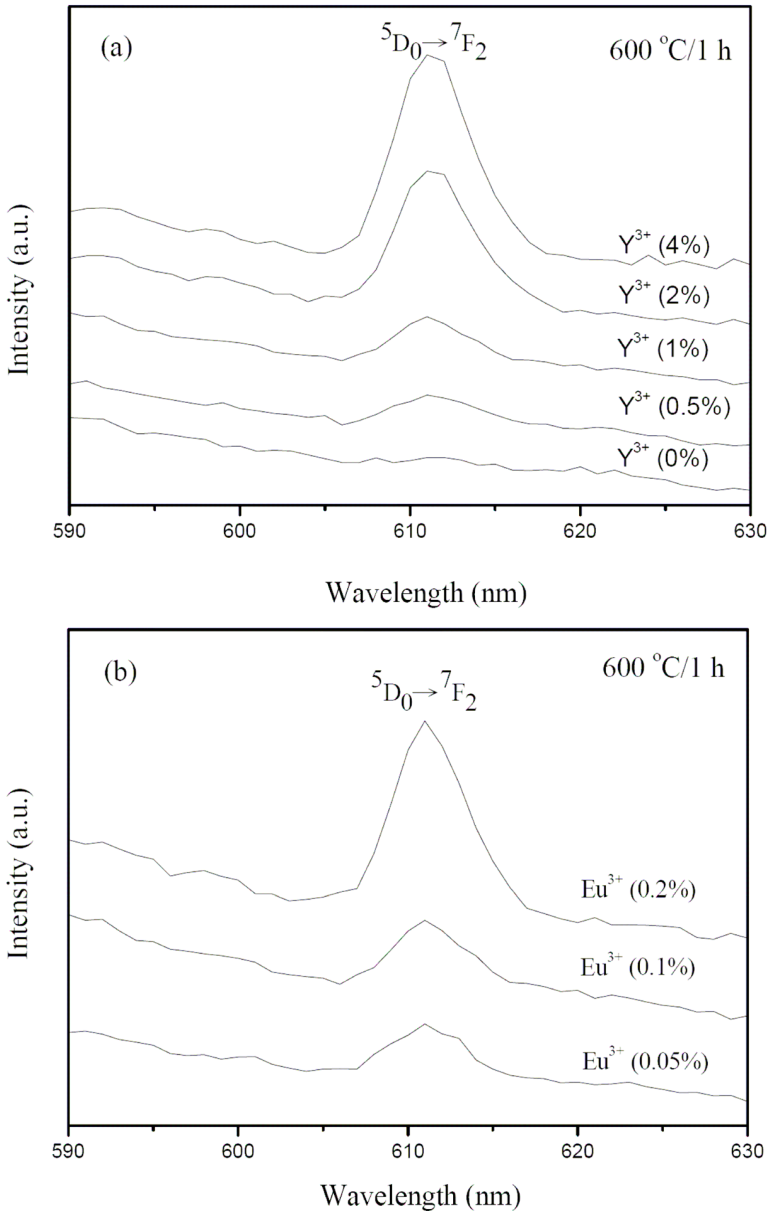


Figure 2: Emission fluorescence spectra of (a) Eu³⁺ (0.1 mol%)-Y³⁺ (0, 0.5, 1, 2, and 4 mol%) and (b) Eu³⁺ (0.05, 0.1, and 0.2 mol%)-Y³⁺ (1 mol%) codoped ITO thin films annealed at 600°C for 1 h.

Eu^{3+} ions, i.e., no inversion symmetry. Similar spectral structure is also observed in other Eu^{3+} -doped amorphous materials.

The more Eu^{3+} or Y^{3+} doping concentrations can increase the PL intensity, as shown in Fig. 2 (a) and (b). Because the Eu^{3+} (0.05, 0.1, and 0.2 mol%)- Y^{3+} (0, 0.5, 1, 2, and 4 mol%) codoped ITO thin films annealed at 600°C for 1 h could be composed of the mixture of amorphous $\text{Eu}_x\text{Y}_y\text{Sn}_{2-x-y}\text{O}_7$ and crystallized $\text{In}_{2-z}\text{Sn}_z\text{O}_{3-\delta}$ phases, Eu^{3+} ions replace Y^{3+} ions and are located at the Y^{3+} site in $\text{Y}_2\text{Sn}_2\text{O}_7$. The more Y^{3+} ions doped, the more $\text{Y}_2\text{Sn}_2\text{O}_7$ formed, which results in the more Eu^{3+} ions can be dissolved in the $\text{Y}_2\text{Sn}_2\text{O}_7$ lattice to reduce the concentration quenching effect and increase the PL intensity.

The excitation spectrum corresponding to the ${}^5\text{D}_0 \rightarrow {}^7\text{F}_2$ transition of Eu^{3+} ion in Eu^{3+} - Y^{3+} codoped ITO thin films annealed at 600°C for 1 h is shown in Figure 3. The broad bands with wavelengths from 350 to 500 nm are ascribed to the f-f transitions of the Eu^{3+} ions [17]. Within this broad band, a sharp and strong band at 465 nm can be assigned to the ${}^7\text{F}_0 \rightarrow {}^5\text{D}_2$ transition. Additionally, because the band gap energy of In_2O_3 nanocrystal is ~ 4 eV (~ 300 nm) which is larger than the bulk In_2O_3 (3.7 eV; ~ 335 nm), a very small excitation band at 300 nm could be attributed to the energy-transfer transition between Eu^{3+} and $\text{In}_{2-z}\text{Sn}_z\text{O}_{3-\delta}$ [18]. The existence of the excitation band corresponding to the band gap energy is the evidence of energy transfer from the $\text{In}_{2-z}\text{Sn}_z\text{O}_{3-\delta}$ nanocrystal to the Eu^{3+} ions but the very small $\text{In}_{2-z}\text{Sn}_z\text{O}_{3-\delta}$ host band in the excitation spectrum of Eu^{3+} indicates that there is a little energy transfer from the $\text{In}_{2-z}\text{Sn}_z\text{O}_{3-\delta}$ host to the doped Eu^{3+} ions.

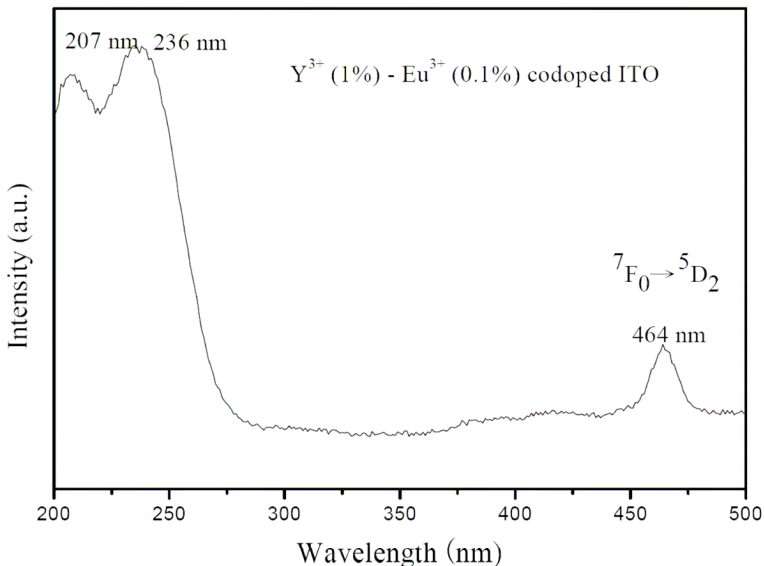


Figure 3: Excitation spectrum corresponding to the ${}^5\text{D}_0 \rightarrow {}^7\text{F}_2$ transition of Eu^{3+} ion in Eu^{3+} - Y^{3+} codoped ITO thin films annealed at $600^\circ\text{C}/1$ h.

On the other hand, the spectrum consists of two very strong broad peaks centered at 207 and 236 nm. It is well known that the charge-transfer transition between Eu^{3+} and O^{2-} generally occur at 250–260 nm. L.R. Singh reported that because the covalency of Eu-O bonds in Y_2O_3 nanocrystals increases, the Eu-O charge transfer energy can be blue shifted in comparison with that of bulk Y_2O_3 [19]. In our system, the average crystal size of Eu^{3+} - Y^{3+} codoped ITO thin films annealed at 600°C for 1 h was ~ 20 nm, which could result in the Eu-O charge transfer energy blue shifting to 236 nm. Moreover, band gap energy of bulk $\text{Y}_2\text{Sn}_2\text{O}_7$ is 4.45 eV (~ 279 eV) but because of quantum confinement effect, the band gap energy of nanosized $\text{Y}_2\text{Sn}_2\text{O}_7$ should be more than 1–2 eV of that value [20]. Therefore, the 207 nm excitation band could be related to the energy-transfer transition between Eu^{3+} and $\text{Y}_2\text{Sn}_2\text{O}_7$ because the $\text{Eu}_x\text{Y}_y\text{Sn}_{2-x-y}\text{O}_7$ is amorphous phase with nanosized crystals.

The above-mentioned results reveal that Eu^{3+} - Y^{3+} codoped ITO thin films annealed at 600°C for 1 h with bixbyite structure can transfer the UV~blue light (200–470 nm) to visible light (611 nm). We believe that Eu^{3+} - Y^{3+} codoped ITO thin films should have good application in the single crystal or poly crystal Si-based solar cells which have less quantum efficiency in the wavelength range from 300 to 500 nm.

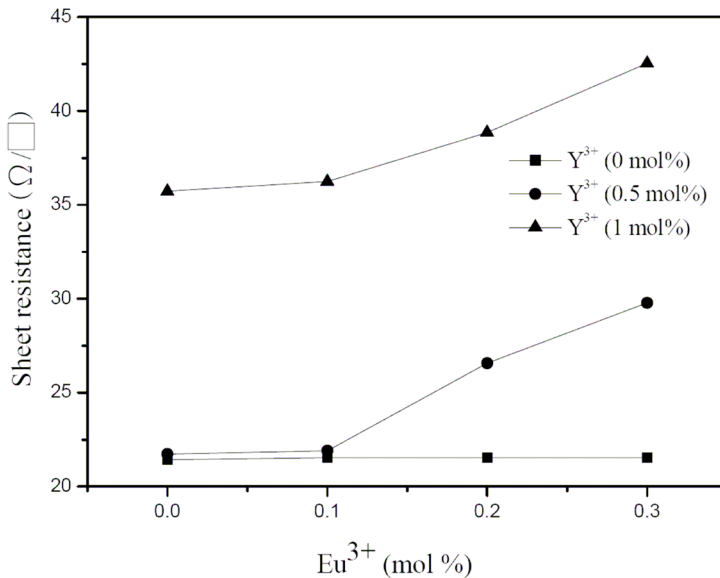


Figure 4: Sheet resistance of Eu^{3+} - Y^{3+} codoped ITO thin films annealed at 600°C for 1 h as a function of different doping concentrations.

3.3 Electrical properties

The sheet resistance of $\text{Eu}^{3+}\text{-Y}^{3+}$ codoped ITO thin films annealed at 600°C for 1 h as a function of different $\text{Eu}^{3+}\text{-Y}^{3+}$ doping concentrations is illustrated in Fig. 4. The resistivity of ITO thin films increased up to $\sim 5\%$ by light Y^{3+} or Eu^{3+} doping concentration (0.5 mol%). However, higher doping concentrations can significantly deteriorate the conductivity. For example, for only 1% Y^{3+} doping concentration the resistivity of ITO thin film was approximately doubled. The addition of Eu^{3+} and Y^{3+} ions into ITO lattice can induce the formation of amorphous pyrochlore phase $\text{Eu}_x\text{Y}_y\text{Sn}_{2-x-y}\text{O}_7$, an insulator with the energy gap of 4.46 eV, which results in the increase of resistivity. [20] Furthermore, because Y^{3+} and Eu^{3+} ions can react with Sn^{4+} ions to form the pyrochlore phase $\text{Eu}_x\text{Y}_y\text{Sn}_{2-x-y}\text{O}_7$, the Sn^{4+} content in $\text{In}_{2-z}\text{Sn}_z\text{O}_{3-\delta}$ should be reduced, which also results in the decrease of the carriers created by the dopant and the increase of resistivity.

According to the above-mentioned investigations of luminescence and resistivity properties, the result reveals that there exists a kind of tradeoff between the luminescence and conductivity. It is hard to achieve a $\text{Eu}^{3+}\text{-Y}^{3+}$ codoped ITO transparent conductive electrode with both of the high luminescent and high conductivity properties. The Eu^{3+} and Y^{3+} codoping concentration should be less than $\sim 0.5\%$ in order to avoid the serious deterioration of conductivity.

4 Conclusions

Eu^{3+} and Y^{3+} ions were codoped into the tin-doped indium oxide transparent conductive electrode to make it possess visible luminescent and conductive properties. The $\text{Eu}^{3+}\text{-Y}^{3+}$ codoped ITO transparent conductive thin films with the precise control on the desired stoichiometry of dopants were fabricated by sol-gel spin-coating technologies. The $\text{Eu}^{3+}\text{-Y}^{3+}$ codoped ITO thin films annealed at 600°C for 1 h could be composed of the mixture of amorphous $\text{Eu}_x\text{Y}_y\text{Sn}_{2-x-y}\text{O}_7$ and crystallized $\text{In}_{2-z}\text{Sn}_z\text{O}_{3-\delta}$ phases, which results in 611 nm visible luminescence. However, no PL can be detected in Eu^{3+} -doped ITO thin films. The higher Y^{3+} concentration can increase the PL intensity because of the formation of more $\text{Eu}_x\text{Y}_y\text{Sn}_{2-x-y}\text{O}_7$. On the other hand, the Eu^{3+} and Y^{3+} codoping concentrations should be controlled within $\sim 0.5\%$ to avoid the deterioration of conductivity. The $\text{Eu}^{3+}\text{-Y}^{3+}$ codoped ITO thin films should be a good solution as the luminescent solar concentrators to convert the 350~465 nm excited light to 611 nm for the enhancement of solar cell efficiency.

Acknowledgement

The authors would like to thank the National Science Council of the Republic of China for financially supporting this research under Contract No. NSC 96-2221-E-194-042-MY2.



References

- [1] Wilkinson, F.J., Farmer, A.J.D. & Geist, J., The near ultraviolet quantum yield of silicon. *Journal of Applied Physics*, 54(2), pp. 1172-1174, 1983.
- [2] Koeppe, R., Sariciftci, N.S. & Buchtemann, A., Enhancing photon harvesting in organic solar cells with luminescent concentrators. *Applied Physics Letters*, 90, 181126, 2007.
- [3] Bailey, S.T., Lokey, G.E. & Hanes, M.S., et al., Optimized excitation energy transfer in a three-dye luminescent solar concentrator. *Solar Energy Materials & Solar Cells*, 91, pp. 67-79, 2007.
- [4] Chatten, A.J., Barnham, K.W.J., Buxton, B.F., Ekins-Daukes, N.J. & Malik, M. A., A new approach to modelling quantum dot concentrators. *Solar Energy Materials & Solar Cells*, 75, pp. 363-371, 2003.
- [5] Reisfeld, R., Prospects of sol-gel technology towards luminescent materials. *Optical materials*, 16, pp. 1-7, 2001.
- [6] Mansour, A.F., El-Shaarawy, M.G., El-Bashir, S. M., El-Mansy, M.K. & Mammam, A qualitative study and field performance for a fluorescent solar collector. *Polymer Testing*, 21, 277-281, 2002.
- [7] Moller, H.J., *Semiconductors for Solar Cells*, Artech House Press, p. 10, 1993.
- [8] Sze, S.M., *Semiconductor Devices: physics and Technology*, Wiley and Sons Inc, 1985.
- [9] Bhatta, P., *Semiconductor Optoelectronic Devices*, Prentice Hall, 1997.
- [10] ASTM JCPDS File No. 44-1087 (In₂O₃), 1997.
- [11] Stock, S.R. & Cullity, B.D., *Elements of X-Ray Diffraction*, Prentice Hall, p. 170, 2001.
- [12] Alam, M.J. & Cameron, D.C., Optical and electrical properties of transparent conductive ITO thin films deposited by sol-gel process. *Thin Solid Films*, 377-378, pp. 455-459, 2000.
- [13] Ambrosini, A., Duarte, A. & Poepelmeier, K.R., Electrical, Optical, and Structural Properties of Tin-Doped In₂O₃-M₂O₃ Solid Solutions (M=Y, Sc). *Journal of Solid State Chemistry*, 153, pp. 41-47, 2000.
- [14] Fujihara, S. & Tokumo, K., Multiband Orange-Red Luminescence of Eu³⁺ Ions Based on the Pyrochlore-Structured Host Crystal. *Chemistry of Materials*, 17, pp. 5587-5593, 2005.
- [15] Park, D.H., Cho, Y.H., Do, Y.R. & Ahn, B.T., Characterization of Eu-Doped SnO₂ Thin Films Deposited by Radio-Frequency Sputtering for a Transparent Conductive Phosphor Layer. *Journal of The Electrochemical Society*, 153(4), pp. H63-H67, 2006.
- [16] Ollier, N., Concas, G., Panczer, G., Champagnon, B. & Charpentier, T., Structural features of a Eu³⁺ doped nuclear glass and gels obtained from glass leaching. *Journal of Non-Crystalline Solids*, 328, pp. 207-214, 2003.
- [17] Nogami, M., Enomoto, T. & Hayakawa, T., Enhanced fluorescence of Eu³⁺ induced by energy transfer from nanosized SnO₂ crystals in glass. *Journal of Luminescence*, 97, pp. 147-152, 2002.



- [18] Dutta, D.P, Sudarsan, V., Srinivasu, P., Vinu, A. & Tyagi, A.K., Indium Oxide and Europium/Dysprosium Doped Indium Oxide Nanoparticles: Sonochemical Synthesis, Characterization, and Photoluminescence Studies. *Journal of Physical Chemistry C*, 112, pp. 6781-6785, 2008.
- [19] Singh, L.R, Ningthoujam, R.S., Sudarsan, V., Srivastava, I., Singh, S.D., Dey, G.K. & Kulshreshtha, S.K., Luminescence study on Eu³⁺ doped Y₂O₃ nanoparticles: particle size, concentration and core-shell formation effects. *Nanotechnology*, 19, 055201, 2008.
- [20] Subramanian, M.A., Aravamudan, G., & Rao, G.V.S., Oxide pyrochlores - A review. *Progress in Solid State Chemistry*, 15, pp. 55-143, 1983.
- [21] Nadaud, N., Lequeux, N., Nanot, M., Jove, J., & Roisnel, T., Structural Studies of Tin-Doped Indium Oxide (ITO) and In₄Sn₃O₁₂. *Journal of Solid State Chemistry*, 135, pp. 140-148, 1998.

